# Analysis of Circulation-Controlled Airfoils in Transonic Flow

F. A. Dvorak* and D. H. Choi†
*Analytical Methods, Inc., Redmond, Washington*

**A method developed for the analysis of the transonic viscous flow over circulation-controlled airfoils is described. A finite-difference method is used to solve the inviscid portion of the flow, and a combination of integral and finite-difference methods is used to calculate the development of the compressible viscous layers. An iterative procedure is employed to give solutions which satisfy the trailing-edge Kutta condition and incorporate the interaction between the viscous and potential regions of the flow. Comparisons between calculated and experimental results show good agreement for surface pressure distributions and lift coefficients over a range of blowing momentum coefficients and Mach numbers.**

## Nomenclature

$a$ = speed of sound
$B$ = $|dz|/|d\sigma|$
$c$ = airfoil chord length
$C_E$ = entrainment coefficient
$C_f$ = skin friction coefficient
$C_l$ = lift coefficient, based on airfoil chord length
$c_p$ = specific heat at constant pressure
$C_p$ = static pressure coefficient
$C_\mu$ = blowing momentum coefficient = $J/\frac{1}{2}\rho U_\infty^2 c$
$E$ = circulation/$2\pi$
$G$ = translated velocity potential
$H, \bar{H}$ = boundary-layer shape factors
$J$ = blowing momentum flux per unit span
$M$ = Mach number
$n$ = coordinate measured normal to the surface
$p$ = static pressure
$q$ = $\sqrt{u^2+v^2}$
$r, \theta$ = coordinates in $\sigma$ plane
$s$ = coordinate measured along the surface
$T$ = temperature
$U, V$ = velocity components in $X$ and $Y$ directions (incompressible flow)
$u, v$ = velocity components in $x$ and $y$ directions (compressible flow)
$X, Y$ = transformed coordinates [Eq. (14)]
$x, y$ = spatial coordinates in Cartesian or body-fitted system
$w$ = complex potential
$z$ = physical plane
$\alpha$ = angle of incidence
$\gamma$ = ratio of specific heats
$\delta$ = boundary-layer thickness
$\delta^*$ = boundary-layer displacement thickness
$\Theta$ = boundary-layer momentum thickness
$\kappa$ = longitudinal curvature of the airfoil
$\Lambda$ = Pohlhausen parameter = $(\delta^2/\nu)(dU_e/dx)$
$\lambda$ = $(\Theta^2/\nu)(dU_e/dx)$
$\nu$ = fluid viscosity
$\rho$ = fluid density
$\sigma$ = computational plane
$\phi$ = velocity potential
$\psi$ = stream function
$\omega$ = $[(T_0+198.6)/(T+198.6)](\sqrt{T_w/T_0})$

*Subscripts*

$e$ = evaluated at the edge of boundary layer
$0$ = stagnation quantities
sepl = separation of lower-surface flow
sepu = separation of upper-surface flow
$t$ = turbulence
tr = transformed
$\infty$ = evaluated at the freestream state

## Introduction

THE application of circulation control by slot blowing about bluff trailing-edge airfoils (Fig. 1) to both fixed- and rotary-wing aircraft has led to improvements in aircraft performance and control. Notable amongst these applications are the Grumman A6 modification[1] and the Kaman circulation-controlled helicopter.[2] The Navy/DARPA X-Wing[3] (Fig. 2) is currently in the advanced development stage leading to a flight demonstrator. Other possible applications of circulation-control technology include the forward swept wing and submarine sternplanes. Airfoils chosen for the three flight demonstration applications were developed at the David W. Taylor Naval Ship Research and Development Center (DTNSRDC) almost exclusively by experiment. No adequate theory existed during the design phase to aid in the airfoil development. Potential flow alone is not sufficient for theoretical analysis, as a valid solution exists for any value of circulation. For a given blowing rate, the actual circulation is a function of the upper- and lower-surface separation points, and only a combined viscid/inviscid procedure can provide this information. Such a method was developed for the Navy and is described in Ref. 4.

This method (program CIRCON) combined an incompressible surface singularity panel method with both integral and finite-difference boundary-layer procedures in an iterative analysis. An initial guess is made for the value of circulation in the potential flow program from which an initial pressure distribution is obtained. The integral laminar transition and turbulent boundary-layer calculation along the lower surface of the airfoil establishes the lower-surface separation point and pressure, $p_{sepl}$. The integral method is also used on the upper surface to provide initial conditions for the finite-difference method. Downstream of the blowing slot, the finite-difference wall jet procedure is used to predict the upper-surface separation pressure level, $p_{sepu}$. The increment in circulation (plus or minus) for the next iteration is a function of the difference in upper- and lower-surface pressure levels. Viscous effects are included in the second and subsequent potential flow calculations via the surface transpiration boundary condition. A converged solution is achieved when both separation pressures are within a prescribed tolerance of each other, and the lift coefficient has converged. CIRCON performed well for a variety of airfoil

Presented as Paper 81-1270 at the AIAA 14th Fluid and Plasma Dynamics Conference, Palo Alto, Calif., June 23-25, 1981; submitted July 16, 1981; revision received May 24, 1982. 

*President. Associate Fellow AIAA.
†Research Scientist. Member AIAA.

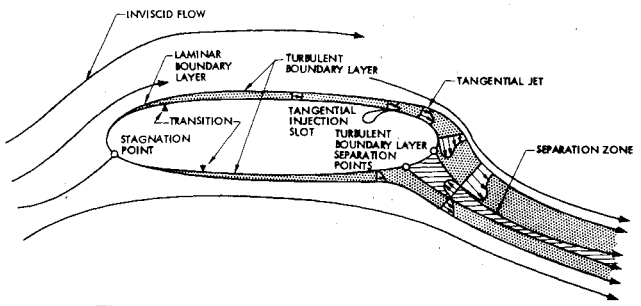


**Fig. 1 Flow over a circulation-controlled airfoil.**

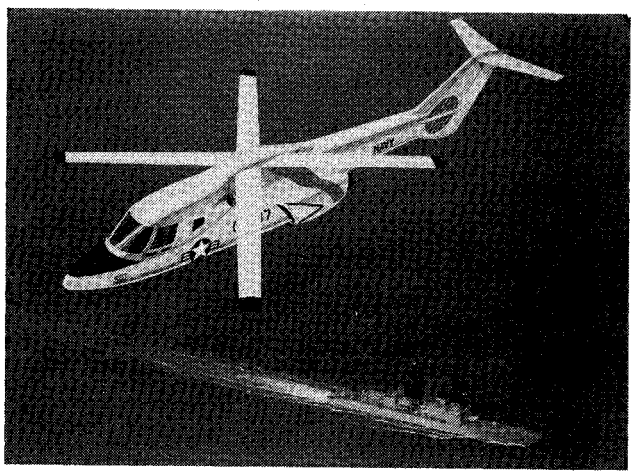

**Fig. 2 X-Wing aircraft concept.**

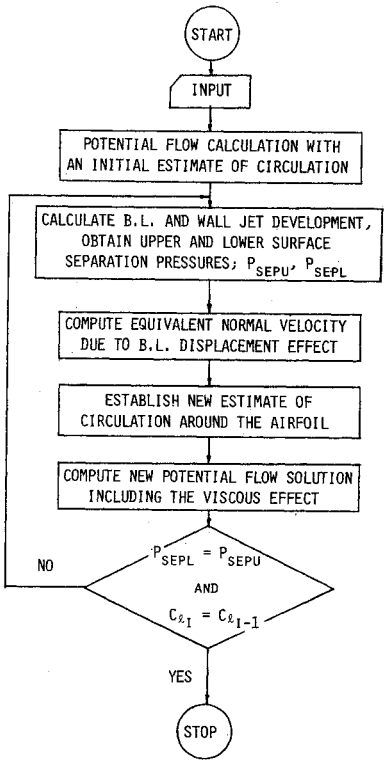


**Fig. 3 Calculation procedure.**

sections as was shown in Ref. 4 and Fig. 8. The method has recently been coupled to an optimization program and is currently being used for low-speed airfoil design.[5]

The X-Wing aircraft as conceived will fly in the fixed-wing mode at speeds in the transonic regime. Because of the generally thicker sections employed for circulation-controlled airfoils, shock waves can be expected. The application of program CIRCON is limited to the subsonic regime; consequently, a transonic version of the program was required. The following sections briefly describe the approach used to develop a transonic analysis procedure.

## Transonic Analysis Method

### General Description

As mentioned in the previous section, the present method, TRACON, basically follows the same procedure as the earlier version, CIRCON.

The flow chart shown in Fig. 3 illustrates the general structure of the code. The computation cycle, that is, the calculation of the potential flow, the boundary layer, the wall jet, and the viscid/inviscid interaction is repeated until the proper convergence criteria are met.

Jameson's transonic flow code,[6] FL06, was adopted with some modification for the potential flow calculation. Here, the exterior of an airfoil is mapped onto the interior of a unit circle so that the entire flowfield can be solved in a finite domain. The equations are solved for the velocity potential $\phi$, with a guessed initial value of circulation; and the velocity field is obtained by simply differentiating $\phi$.

The result is used for the boundary-layer calculation after the array is rearranged starting from the forward stagnation point. The boundary-layer calculation is initiated by the laminar boundary-layer method of Cohen and Reshotko,[7] and is continued on to turbulent boundary layers using Green's "lag-entrainment" method.[8] An improved version of the finite-difference method used in CIRCON is employed for the upper-surface boundary-layer development downstream of the blowing slot for the blowing case.

Having obtained the points of separation and corresponding static pressures, a new value of circulation is estimated on the basis of separation pressures and current value of lift. A new potential flow solution can then be computed using this new estimate of circulation with the viscous effect, i.e., velocity component normal to the surface, taken into account.

Convergence is checked at this stage. The calculation continues for another cycle unless $p_{sepu}$ and $p_{sepl}$ are in close agreement and the variation of the lift coefficient between successive iterations is in the range of convergence.

Details of individual elements are fully described in the following sections.

### Potential Flow Calculation Method

*Basic Equations*

From the equation of continuity and the momentum equation, we have

$$(a^2-u^2)\frac{\partial u}{\partial x}-uv\left(\frac{\partial u}{\partial y}+\frac{\partial v}{\partial x}\right)+(a^2-v^2)\frac{\partial v}{\partial y}=0 \qquad (1)$$

Assuming irrotational flow, a velocity potential, $\phi$, can be defined; i.e.,

$$u=\frac{\partial \phi}{\partial x} \qquad v=\frac{\partial \phi}{\partial y} \qquad (2)$$

Substitute these into Eq. (1) to obtain

$$(a^2-u^2)\phi_{xx}-2uv\phi_{xy}+(a^2-v^2)\phi_{yy}=0 \qquad (3)$$

This equation can be solved for $\phi$ with the use of the energy equation

$$a^2+\frac{\gamma-1}{2}q^2=\left(\frac{1}{M_\infty^2}+\frac{\gamma-1}{2}\right)q_\infty^2 \qquad (4)$$

where

$$q=\sqrt{u^2+v^2}$$

The Neumann boundary condition is prescribed along the surface; $\partial\phi/\phi n=0$ is set initially, and it takes a new value which reflects the viscous effect after each cycle of iteration: first iteration,

$$\frac{\partial\phi}{\partial n}=0 \tag{5a}$$

subsequent iterations,

$$\frac{\partial\phi}{\partial n}=\frac{1}{\rho}\frac{\partial}{\partial s}(\rho u\delta^*)=f \tag{5b}$$

where $\delta^*$ is the boundary-layer displacement thickness and $s$ is measured along the airfoil surface.

Because of the nature of Eq. (3), hyperbolic if the local Mach number $M=q/a>1$ and elliptic if $M<1$, it is essential to transform the infinite flowfield onto a finite domain. This can be achieved by mapping of the exterior of the airfoil in the $z$ plane conformally onto the interior of a unit circle in the $\sigma$ plane.

This transformation is particularly useful because an evenly distributed grid system in the circle plane gives denser finite mesh near the body at the leading and trailing edges in the physical plane where it is needed most.

*Mapped Coordinate System*

Consider the speed in the $z$ plane,

$$q^2=u^2+v^2=\left|\frac{\partial\phi}{\partial z}\right|^2=\left|\frac{\partial\phi}{\partial\sigma}\right|/B^2=\frac{1}{B^2}\left[\left(\frac{\partial\phi}{r\partial\theta}\right)^2+\left(\frac{\partial\phi}{\partial r}\right)^2\right] \tag{6}$$

where

$$B=\left|\frac{\partial z}{\partial\sigma}\right|$$

Thus we have

$$\frac{\partial\phi}{\partial x}=\frac{\partial\phi}{r\partial\theta}/B \qquad \frac{\partial\phi}{\partial y}=\frac{\partial\phi}{\partial r}/B \tag{7}$$

The complex potential about a unit circle in a uniform stream is given by

$$w=U_\infty(z+1/z)+iE\ell nz \tag{8}$$

Here the velocity potential at infinity becomes unbounded and is on the order of $r$. Since the present transformation requires the direct inversion of this external flow, the singular behavior at infinity inevitably occurs at the origin of the $\sigma$ plane.

In order to remove this singularity at the origin, $0(1/r)$, and the discontinuity at $\theta=2\pi$ due to the circulation, a translated potential, $G$, is introduced:

$$G=\phi-[\cos(\theta+\alpha)/r]+E(\theta+\alpha) \tag{9}$$

where $2\pi E$ is the circulation, and $\alpha$ is the angle of attack.

Substituting Eqs. (7) and (9) into Eq. (2) to obtain

$$(a^2-u^2)G_{\theta\theta}-2uvrG_{r\theta}+(a^2-v^2)r\frac{\partial}{\partial r}\left(rG_r\right)$$
$$-2uv(G_\theta-E)+(u^2-v^2)G_r$$
$$+(u^2+v^2)\left(\frac{u}{r}B_\theta+vB_r\right)=0 \tag{10}$$

where

$$u=\frac{r(G_\theta-E)-\sin(\theta+\alpha)}{B}$$

$$v=\frac{r^2G_r-\cos(\theta+\alpha)}{B}$$

the Neumann boundary condition reduces to

$$G_r=\cos(\theta+\alpha)-f/B \qquad \text{at } r=1 \tag{11}$$

while the far-field boundary condition becomes

$$G=E\{\theta+\alpha-\tan^{-1}[\sqrt{1-M_\infty^2}\tan(\theta+\alpha)]\} \qquad \text{at } r=0 \tag{12}$$

Here, the circulation constant $E$ is determined by the Kutta condition derived from the upper- and lower-surface separation pressures and is discussed in a later section.

*Method of Solution*

The transformed Eq. (10) with boundary conditions, Eqs. (11) and (12), is solved by a finite-difference scheme. Upwind differencing is used where the local flow is supersonic, while central difference formulas are used at subsonic points. The resulting set of difference equations is solved iteratively. Details of the method are referred to in the original paper[6] and will not be reproduced here.

After the translated potential $G$ is obtained, the tangential velocity component u on the surface can be obtained readily through simple differencing. The pressure coefficient $C_p$ along the surface is given by

$$C_p=\frac{1}{(\gamma/2)M_\infty^2}\left\{\left[1+\frac{\gamma-1}{2}M_\infty^2(1-u^2)^{\gamma/\gamma-1}\right]-1\right\} \tag{13}$$

The pressures at the off-body points, which are necessary for the wall jet development calculation, can be obtained with little extra effort since $G$ has been determined for the entire flowfield.

The method was tested thoroughly during the course of this work and found to be quite satisfactory. With 64 points around the body and 16 points in the radial direction, it converged within $10^{-6}$ in less than ten iterations for most cases. Shock locations, if there are any, are predicted quite accurately.

*Calculation of Boundary-Layer Development*

The boundary-layer development along upper and lower surfaces are calculated by using Cohen-Reshotko's laminar boundary-layer calculation method and Green's turbulent boundary-layer calculation method. The Granville procedure is adopted as a transition criterion[9] and the possibility of the reattachment as a turbulent boundary layer after laminar boundary-layer separation is also examined on the basis of the Reynolds number based on the momentum thickness at the point of separation.[9]

*Cohen and Reshotko Method*

This integral method was developed for the steady two-dimensional laminar boundary layer with the assumption that the surface temperature is uniform.

First, consider the Stewartson transformation,

$$\frac{\partial\psi}{\partial y}=\frac{\rho u}{\rho_0} \qquad \frac{\partial\psi}{\partial x}=\frac{-\rho v}{\rho_0} \qquad X=\int_0^x\omega\frac{a_e}{a_0}\frac{p_e}{p_0}\,dx$$

$$Y=\frac{a_e}{a_0}\int_0^y\frac{\rho}{\rho_0}\,dy \qquad U=\frac{\partial\psi}{\partial y} \qquad V=-\frac{\partial\psi}{\partial x} \tag{14}$$

where $\psi$ and $a$ represent the stream function and the speed of sound, respectively. Capital letters denote quantities of the equivalent incompressible problem. With this transformation, the equivalent incompressible problem can be formulated.

The momentum integral equation in two-dimensional flow is given by

$$\frac{d\Theta_{tr}}{dX} + \frac{\Theta_{tr}}{U_e}\frac{dU_e}{dX}(H_{tr}+2) = \frac{C_f}{2} \tag{15}$$

where $C_f$ is the skin friction coefficient $\tau_w/\frac{1}{2}\rho U_e^2$, and the subscript tr denotes the transformed (incompressible) coordinate. Introducing a parameter, $\lambda$, where

$$\lambda = \frac{\Theta_{tr}^2}{\nu_0}\frac{dU_e}{dX} \tag{16}$$

and substituting this into Eq. (15) gives

$$U_e\frac{d}{dX}\left[\frac{\lambda}{dU_e/dX}\right] = 2\left[-\lambda(H_{tr}+2) + \frac{C_f}{2}\frac{U_e\Theta_{tr}}{\nu}\right] \tag{17}$$

The right-hand side of this equation can be approximated by a linear function of $\lambda$[7,10]; i.e., $C_1 - C_2\lambda$, and, therefore, the ordinary differential equation (17) has an analytical solution:

$$\lambda = C_1 U_e^{-C_2}\frac{dU_e}{dX}\int_0^X U_e^{C_2-1}dX \tag{18}$$

where the arbitrary constant vanishes to ensure a finite-momentum thickness at the stagnation point. The Stewartson tranformation of Eqs. (14) finally leads us to

$$\lambda = C_1 M_e^{-C_2}\frac{dM_e}{dx}T_e^{-4}\int_0^x M_e^{C_2-1}T_e^4 dx \tag{19}$$

This can be readily solved for $\lambda$ by simple integration formulas such as the trapezoidal rule. Then the momentum thickness and the shape factor $H$ are obtained from the explicit expressions of $\lambda$. (See Ref. 7 for the details.)

The separation of the boundary layer is detected by examining the Pohlhausen parameter, $\Lambda = (\delta^2/\nu)(dU_e/dx)$, assuming that the $H-\Lambda$ table for the incompressible flow is still valid.

After transition, either through natural transition or through a separation/reattachment process, Green's method takes over the calculation of downstream turbulent boundary-layer development.

*Green's Method*

This is a "lag-entrainment" integral method involving three equations: momentum-integral, entrainment, and a rate equation for the entrainment coefficient.[8] The method is a combination of Head's original entrainment momentum-integral method and the turbulent model proposed by Bradshaw et al. in which the algebraic relation for the entrainment coefficient of Head's method is replaced by a rate equation derived from the turbulent kinetic energy equation.

The resulting equations are

$$\frac{d\Theta}{dx} = F_1(\Theta, \bar{H}, C_E) \tag{20}$$

$$\frac{d\bar{H}}{dx} = F_2(\Theta, \bar{H}, C_E) \tag{21}$$

$$\frac{dC_E}{dx} = F_3(\Theta, \bar{H}, C_E) \tag{22}$$

where

$$\Theta = \int_0^\infty \frac{\rho u}{\rho u_e}\left(1-\frac{u}{u_e}\right)dy$$

$$\bar{H} = \frac{1}{\Theta}\int_0^\infty \frac{\rho}{\rho_e}\left(1-\frac{u}{u_e}\right)dy$$

$$C_E = \frac{1}{\rho_e u_e}\frac{d}{dx}\int_0^\delta \rho u dy$$

This system of ordinary differential equations is solved by the Runge-Kutta method. The separation point can be located by monitoring both the friction coefficent $C_f$ and the shape factor $H$.

**Calculation Method for the Wall Jet**

The downstream section of the blowing slot is treated using a finite-difference scheme of the Crank-Nicholson type. The second-order equations of $x$ momentum and temperature are used to solve this complicated flow. The pressure variation across the boundary layer is obtained from the potential flow solution and is used as a forcing term in the calculation; $x$-momentum equation:

$$\frac{\rho u}{1+\kappa y}\frac{\partial u}{\partial y} + \left[\rho v - \frac{2\kappa}{1+\kappa y}(\mu+\rho\nu_t)\right]\frac{\partial u}{\partial y} + \frac{v\kappa}{1+\kappa y}u - \frac{\partial}{\partial y}\left[(\mu+\rho\nu_t)\frac{\partial u}{\partial y}\right] + \frac{1}{1+\kappa y}\frac{\partial p}{\partial x} = 0 \tag{23}$$

energy equation:

$$\frac{\rho u c_p}{1+\kappa y}\frac{\partial T}{\partial x} + c_p\rho v\frac{\partial T}{\partial y} - \frac{u}{1+\kappa y}\frac{\partial p}{\partial x} - \frac{\partial}{\partial y}\left[\left(K+\frac{\rho\nu_t}{Pr_t}\right)\frac{\partial T}{\partial y}\right] = 0 \tag{24}$$

continuity equation:

$$\frac{1}{1+\kappa y}\frac{\partial(\rho u)}{\partial x} + \frac{\partial(\rho v)}{\partial y} + \rho\kappa v = 0 \tag{25}$$

where $K$ is the heat conductivity, $\kappa$ is the longitudinal curvature of the airfoil, and $\rho v = \rho v + \rho' v'$.

The closure relationship used the eddy viscosity model originally generated by Prandtl and later modified by Sawyer (see Refs. 4 and 11)

$$-\overline{u'v'} = \nu_t\left(\frac{\partial u}{\partial y} - C\frac{u\kappa}{1+\kappa y}\right) \tag{26}$$

where $C$ is an explicit function of $y$.

Equations (23) and (24) can be solved by marching in the $x$ direction provided that an initial velocity profile is known. The outer part of this profile is obtained from Thompson's two-parameter profile family[12] by using $R_\Theta$ and $H$, which are available from the upstream boundary-layer calculation. The wall jet region is made up of a laminar boundary layer at the wall blending to a computed inviscid velocity distribution in the core.

After finite differencing, Eqs. (23) and (24) will form tridiagonal matrix equations and these linear systems are solved sequentially until they converge. The normal velocity, $v$, is updated through integrating the continuity equation. If the solution fails to converge within five iterations, the current step size is reduced by half and the solution is sought at this new $x$ station.

The procedure is continued until the boundary layer separates. If a negative velocity is detected somewhere other than at the wall surface, the region above this point is dropped from the computation domain and the calculation is carried on to the wall separation point.

#### Viscous/Potential Flow Interaction

The effect of the viscous layer is incorporated in the next potential flow calculation in the form of a normal velocity component along the surface; i.e.,

$$v(s) = \frac{1}{\rho}\frac{\partial}{\partial s}(\rho u \delta^*) \tag{27}$$

which was derived under the assumption of inviscid flow adjacent to the surface.

A new estimate of circulation is now established according to the predicted upper- and lower-surface separation pressures $p_{sepu}$ and $p_{sepl}$, respectively,

$$E_{i+1} = E_i + k(C_{p_{sepu}} - C_{p_{sepl}}) \tag{28}$$

where $2\pi E$ is the circulation and the numerical constant $k$ has a value in the range $0.2 \leq k \leq 0.3$.

#### Aerodynamic Forces

The lift and pitching moment coefficients are obtained from the calculated pressure distribution, and the drag is determined through direct integration of the skin friction and pressure around the contour of the airfoil.

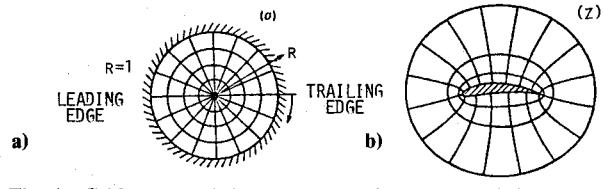


**Fig. 4 Grid system: a) in the computational plane; b) in the physical plane.**

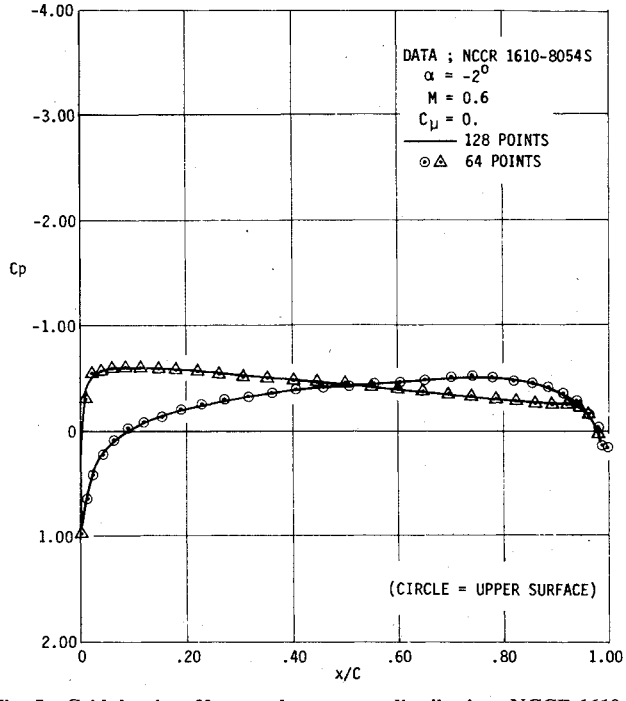


**Fig. 5 Grid density effect on the pressure distribution; NCCR 1610-8054S.**

## Discussion of Results

A numerical test was made to determine grid density effect on the potential flow solution. In Fig. 5, two sets of pressure distributions are presented: one was obtained with 128 points and the other with 64 points used to represent the airfoil contour, with good agreement between them. This suggests that a 64-point grid system is sufficient for the present purposes although a denser grid system is expected to give more accurate shock locations. From here on, all calculations were made with the grid distribution of 64 points around and 16 points normal to the airfoil.

The method has been tested thoroughly against experimental data. The data, which were collected by NSRDC on the NSRDC two-dimensional airfoils, NCCR 2520-7067N and NCCR 1610-8054S, the profiles of which are shown in Fig. 6, for a wide range of blowing momentum coefficients, were used extensively for this purpose. The section, NCCR 1510-7067N, has a circular trailing edge whereas the trailing edge of the transonic airfoil, NCCR 1610-8054S, is a log-

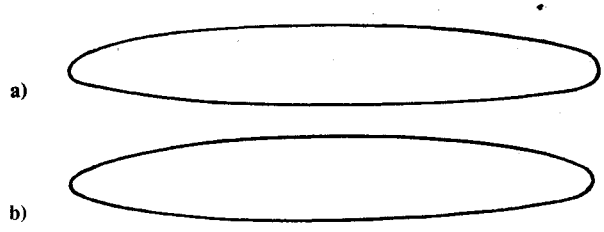


**Fig. 6 Airfoil geometry. a) NCCR 1510-7067N, b) NCCR 1610-8054S.**

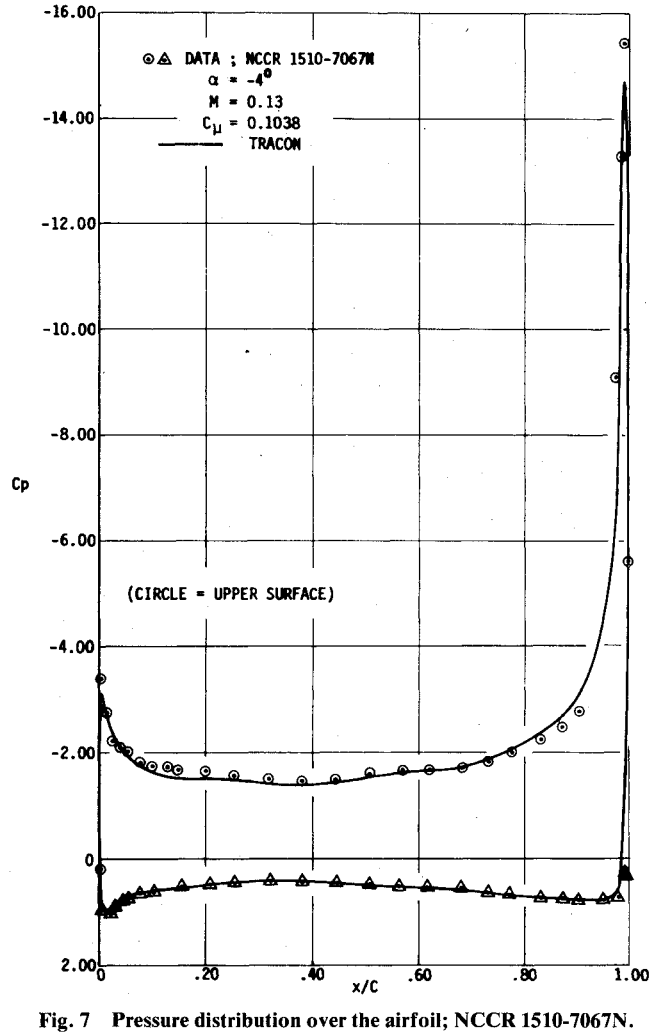


**Fig. 7 Pressure distribution over the airfoil; NCCR 1510-7067N.**

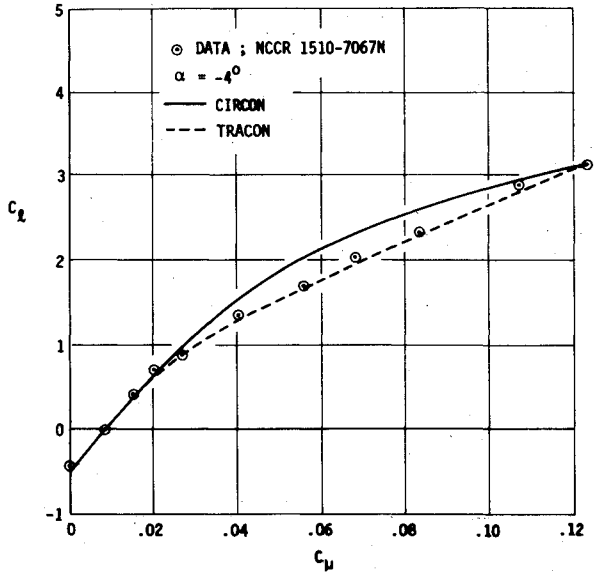


Fig. 8 Comparison between calculated and measured lift coefficier for a range of momentum coefficients; NCCR 1510-7067N.

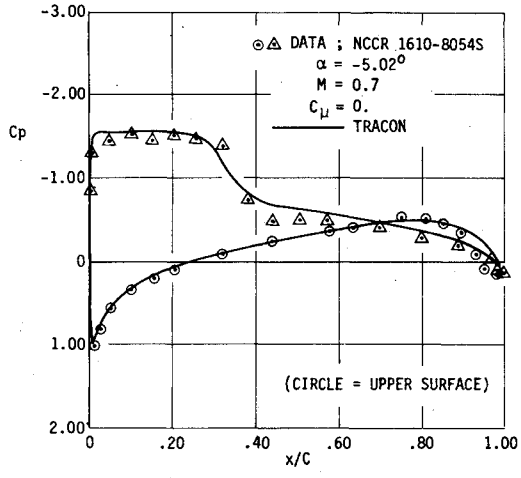


Fig. 9 Pressure distribution over the airfoil; NCCR 1610-8054S.

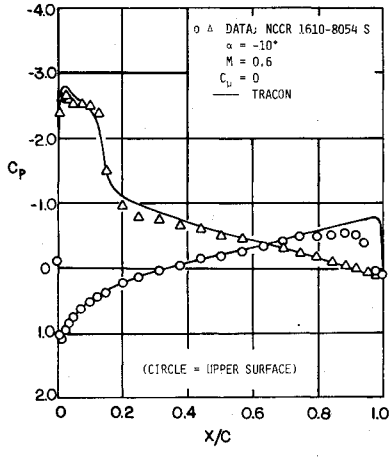


Fig. 10 Pressure distribution over the airfoil; NCCR 1610-8054S.

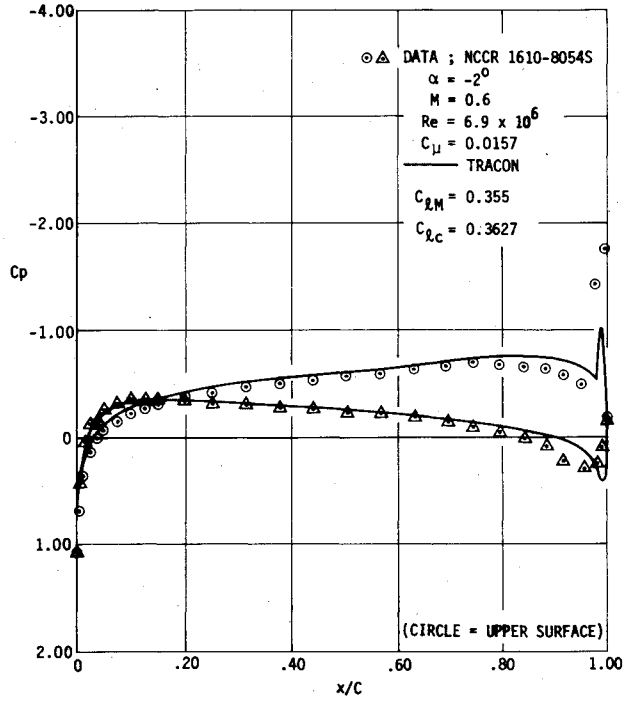


Fig. 11 Pressure distribution over the airfoil; NCCR 1610-8054S.

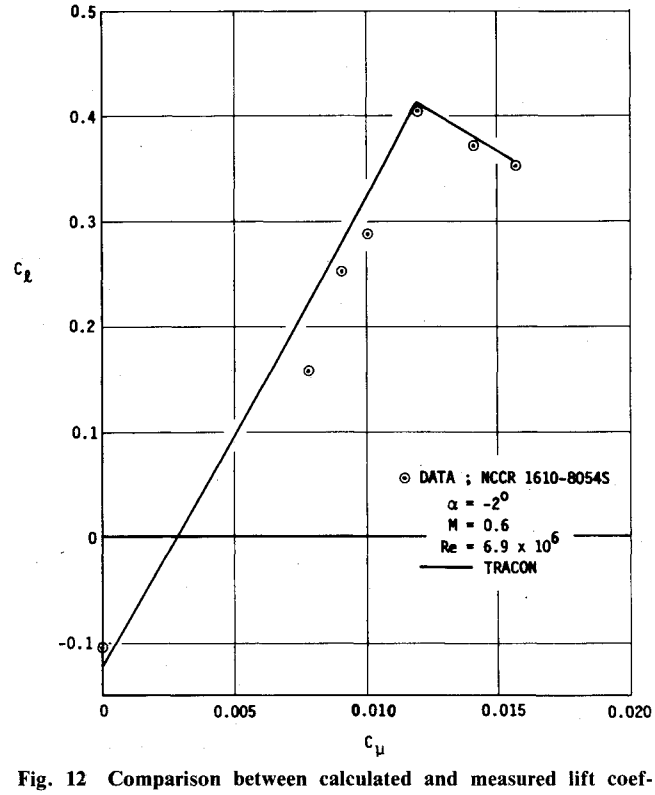


Fig. 12 Comparison between calculated and measured lift coefficients for a range of momentum coefficients; NCCR 1610-8054S.

spiral. The blowing slots of NCCR 1510-7067N and NCCR 1610-8054S are located at 96.8% and 98% of the chord, respectively. Figures 7 and 8 show the results at low Mach number for the NCCR 1510-7067N and are in excellent agreement with the data. Figure 8 also shows an improvement in the calculation method over the previous version, CIRCON. A high Mach number ($M=0.7$) flow without blowing, in which a shock is present, is shown in Fig. 9. The location of the shock is well predicted, and the overall pressure distribution is satisfactory. A more severe case is shown in Fig. 10, and again the shock strength and location are well represented. The upper surface pressures in the trailing-edge region are not as well predicted. A probable explanation involves the manner in which the airfoil is represented downstream of the slot. The analysis requires a smooth contour; consequently the slot region is faired in, resulting in

slightly different contours between experiment and analysis.

Figure 11 shows a pressure distribution for the NCCR 1610-8054S. Mach number and angle of attack are approximately 0.6 and $-2$ deg, respectively. The agreement, in general, is quite good, although the method has some difficulty in predicting the pressure accurately in the region of the blowing slot. For this case, the blowing coefficient is of sufficient magnitude that the slot flow is choked. Downstream of the slot the flow can have an embedded shock structure due to the initially underexpanded jet. The analysis procedure currently is not capable of treating this feature of the flow.

Finally, the $C_l - C_\mu$ curve for this case is shown in Fig. 12, and the result is very encouraging. As in the experimental data, the lift increases as $C_\mu$ increases until it reaches the maximum and then begins to drop in spite of the continuous increase in $C_\mu$. It is evident from the experiment that the drop in $C_l$ is due to the presence of shock induced by strong slot blowing. At the present time, the analysis method is not capable of predicting the presence of this shock. However, with the present wall jet model, for $\Delta C_p$, which is based on Kind's measurements,[13] the method is able to predict the optimum blowing momentum coefficient, $C_\mu$, and the corresponding lift coefficient, $C_l$.

## Conclusions

Comparisons with experiment indicate that the new method gives results as good if not better than CIRCON in subsonic flow. In the transonic regime, the method is capable of predicting shock locations quite well, particularly for rounded trailing-edge airfoils at zero blowing coefficient. This is believed to be currently a unique capability. At the higher blowing coefficients where jet-induced shocks are present, additional work is needed to enable the analysis to predict the optimum blowing coefficient for a given Mach number and angle of attack, although this may be a fortuitous result of the model used to determine the additional suction due to jet effects.

## Acknowledgments

This work was supported by the David W. Taylor Naval Ship Research and Development Center of the U.S. Navy under Contracts N00167-79-C-0098 and N00167-81-C-0041. This support is gratefully acknowledged.

## References

[1] Englar, R.J., "Investigation into and Application of the High Velocity Circulation Control Wall Jet for High Lift and Drag Generation on STOL Aircraft," AIAA Paper 74-502, Palo Alto, Calif., June 1974.

[2] Wilkerson, J.B., Reader, K.R., and Linck, D.W., "The Application of Circulation Control Aerodynamics to a Helicopter Rotor Model," *Journal of the American Helicopter Society,* Vol. 19, April 1974, pp. 1-16.

[3] Williams, R.M., "Application of Circulation Control Rotor Technology to a Stopped Rotor Aircraft Design," Paper presented at the First European Rotorcraft and Powered Lift Aircraft Forum at Southampton, England, Sept. 1975.

[4] Dvorak, F.A. and Kind, R.J., "Analysis Method for Viscous Flow over Circulation-Controlled Airfoils," *Journal of Aircraft,* Vol. 16, Jan. 1979, pp. 23-28.

[5] Tai, T.C., Kidwell, G.H., and Vanderplaats, G.W., "Numerical Optimization of Circulation Control Airfoils," Paper 81-0016 presented at the AIAA 9th Aerospace Sciences Meeting, St. Louis, Mo., Jan. 1981.

[6] Jameson, A., "Numerical Computation of Transonic Flows with Shock Waves," in *International Union of Theoretical and Applied Mechanics,* Springer-Verlag, New York, 1975, pp. 384-414.

[7] Brune, G.W. and Manke, J.W., "An Improved Version of the NASA Lockheed Multi-Element Airfoil Analysis Computer Program," NASA CR-154323, March 1978, pp. 69-87.

[8] Green, J.E., Weeks, D.J., and Brooman, J.W.F., "Prediction of Turbulent Boundary Layers and Wakes in Compressible Flow by a Lag-Entrainment Method," Royal Aircraft Establishment TR-52231, Dec. 1972.

[9] Dvorak, F.A. and Woodward, F.A., "A Viscous/Potential Flow Interaction Analysis Method for Multi-Element Infinite Swept Wings," Vol. I, NASA CR-2476, Nov. 1974.

[10] Thwaites, B., "Approximate Calculation of the Laminar Boundary Layer," Aeronautical Quarterly, Vol. 1, 1949, pp. 245-280.

[11] Dvorak, F.A., "Calculation of Turbulent Boundary Layers and Wall Jets over Curved Surfaces," *AIAA Journal,* Vol. 11, April 1973, pp. 517-524.

[12] Thompson, B.G.J., "A New Two-Parameter Family of Mean Velocity Profiles for Incompressible Turbulent Boundary Layers on Smooth Walls," ARC R&M 3464, 1965.

[13] Kind, R.J., "A Proposed Method of Circulation Control," Ph.D. thesis, Cambridge University, Cambridge, England, 1967.